Supporting Information

Bench-Top Fabrication of Single-Molecule Nanoarrays by DNA Origami Placement

Rishabh M. Shetty[a,b,e,*], **Sarah R. Brady**[a], **Paul W. K. Rothemund**[c], **Rizal F. Hariadi**[a,d,1,*], **and Ashwin Gopinath**[c,e,1,*]

[a]Biodesign Center for Molecular Design and Biomimetics (at the Biodesign Institute) at Arizona State University, Tempe, AZ 85287, USA.; [b]School of Biological and Health Systems Engineering, Arizona State University, Tempe, AZ 85287, USA.; [c]Departments of Bioengineering, Computational and Mathematical Sciences, and Computation and Neural Systems, California Institute of Technology, Pasadena, CA 91125, USA.; [d]Department of Physics, Arizona State University, Tempe, AZ 85287, USA.; [e]Department of Mechanical Engineering, Massachusetts Institute of Technology, Cambridge, MA 02139, USA.

[1]A.G. and R.F.H. supervised this work equally.

[*]To whom correspondence should be addressed. E-mail: rmshetty@asu.edu, rhariadi@asu.edu, and agopi@mit.edu

Contents

S1. Materials and Methods

DNA origami design, preparation and purification.

caDNAno file and supplementary files. The caDNAno design file, list of staples, a staple map, as well as a supplementary movie of raw DNA–PAINT data are included as a zip archive: `Origami designs+staples+movie.zip`.

Design. A circular origami with a square hole was designed using caDNAno http://cadnano.org/ as detailed by Gopinath *et al.*[59] To control the face of the origami that binds to the binding site, we position all staple ends on the same face of the origami so that single-stranded 20`T` extensions to 5′ staple ends would all project from the same face of the origami.

Preparation. Staple strands (Integrated DNA Technologies, 640 nM each in water) and the scaffold strand (single-stranded p8064, 100 nM from Tilibit) were mixed together to target concentrations of 100 nM (each staple) and 20 nM, respectively (a 5:1 staple:scaffold ratio) in 40 mM Tris, 20 mM Acetate, and 1 mM Ethylenediaminetetraacetic acid (EDTA) with a typical pH around 8.6, and 12.5 mM magnesium chloride ($MgCl_2$) (1x TAE/Mg^{2+}). 100 μL volumes of staple/scaffold mixture were heated to 90 °C for 5 min, and annealed from 90 °C to 25 °C at 0.1 °C/min in a PCR machine. We used 0.2 mL TempAssure^{TM} tubes (USA Scientific). Once purified, the origami were stored in 0.5 mL DNA LoBind tubes (Eppendorf) to minimize loss of origami to the sides of the tube.

For annealing DNA–PAINT origami, and any other origami annealed overnight, a ramp of 0.004 °C/min was used in the critical "folding" range of 60–50 °C, a 0.005 °C/min ramp was used between 70–60 °C and 50–40 °C, and a 0.1 °C/min ramp was used between the 90–70 °C and 40–25 °C temperature ranges. "Docking strand" staples were introduced at 75–100x excess to the annealing mix.

Purification. A high concentration of excess staples will compete with DNA origami and inhibit DNA origami placement. Thus, origami were purified away from excess staples using 100 kD molecular weight cut-off filters (MWCO) spin filters (Amicon Ultra-0.5 Centrifugal Filter Units with Ultracel-100 membranes, Millipore, UFC510024). By the protocol below, recovery is generally 40–50%, and staples are no longer visible by agarose gel electrophoresis:

1. Wet the membrane of the spin filter by adding 500 μL 1x TAE/Mg^{2+}.
2. Centrifuge at 6000 rcf for 5 min at room temperature (RT), until the volume in the filter is ∼80 μL.
3. Discard the filtrate.
4. Add 100 μL of unpurified origami and 300 μL 1x TAE/Mg^{2+}. Spin at 6000 rcf for 5 min at RT.
5. Discard the filtrate.
6. Add 420 μL 1x TAE/Mg^{2+} and spin at 6000 rcf for 5 min at RT.
7. Repeat step (4) two more times.
8. Invert the filter into a clean tube and spin at 6000 rcf for 5 min at RT to collect purified origami (∼80 μL).

Note In the case of DNA origami annealed with a 75–100x excess of fluorophores (for photobleaching) or DNA–PAINT, spin the filter at 2000 rcf for 15 min 5–7 times before inverting into a new tube to collect the purified product. This is to avoid fluorophores (and associated origami) from sticking to the sides of the filter and adversely affecting the purified origami yield or causing origami aggregation/deformation. Always check the purity of origami using agarose gel electrophoresis (100 V, 1%, 1x TAE, 1 hr).

The total time required for this purification is roughly 30–120 min. Post-purification, origami are quantified using a NanoDrop spectrophotometer (Thermo Scientific), estimating the molar extinction coefficient of the DNA origami as that of a fully double-stranded p8064 molecule (extinction coefficient = 164,568,055 /M/cm). We typically work with stock solutions of 20–30 nM DNA origami (3–5 OD). The working concentration for origami during placement is 100–500 pM, which is too small to be measured with the NanoDrop. Single-origami occupancy is sensitive to origami concentration, therefore, to maintain

consistency for each series of experiments, a single high concentration stock solution (from a single purification) was made and diluted to 100–500 pM, as needed. Origami concentration was optimized for best placement results for each origami stock.

S2. Fabrication of binding sites and origami placement:

Materials and equipment required.

1. 10×10 mm^2 coverslips (Ted Pella, 260375-15).
2. Plasma cleaner (Harrick Basic Plasma Cleaner PDC-32G/PDC-32G-2)
3. Hotplate and stirrer (Denville)
4. Desiccator (Hach, Product no. 223830)
5. Branson ultrasonic bath, AFM (Bruker FastScan).
6. Appropriately sized Polystyrene (PS) microspheres (3000 Series Nanosphere; Size Standards (4000 Series Monosized 1 μm particles 4009A; 700 nm [3700A]; 495 nm [3495A]; and 400 nm [3400A]), Thermo Fisher Scientific).
7. Passivation agent: HMDS (440191–100 mL, Sigma).

Protocol for binding site creation.

1. Isopropanol (IPA) wash for 2 min.
2. Blow dry glass chip with nitrogen.
3. 10–min air plasma cleaning in Harrick plasma cleaner at ∼18 W ("High" setting).
4. In an Eppendorf tube, pour 10 drops (∼360 μL suspension) of 1 μm/700 nm/500 nm/400 nm PS nanospheres. Gently vortex the nanospheres before use.
5. Spin at 8,000–10,000 rpm for 5 min (faster and/or longer spinning for smaller nanosphere sizes).
6. Remove supernatant and add 360 μL of ultrapure water to re-suspend pellet.
7. Spin at 8,000-10,000 rpm for 5 min.
8. Remove supernatant and re-suspend pellet in 25% ethanol and 75% water (∼3.5x more concentrated, *i.e.* 100 μL). Pipette/vortex aggressively to re-suspend all particles (∼$6.5e^{10}$ particles/mL for 1 μm nanospheres at 1% w/w solids).
9. Drop-cast onto activated chip surface and let dry at ∼45° angle at R.T (resting against a glass stirrer or similar object). Cover entire surface (generally requires 5-10 μL for a 10×10 mm^2 chip). Once dried, you should be able to observe a diffraction pattern (crystalline structure) confirming the existence of a close-packed monolayer/multilayer of nanospheres. If unsure, check under a microscope.
10. Heat at 60 °C for 5 min to remove any moisture.
11. 2–min "descum" plasma in air at ∼18 W in Harrickplasma cleaner.
12. In a desiccator, add 8–10 drops of HMDS (in a glass cuvette), and deposit under a vacuum seal for 20 min. This should work equally well in an enclosed petri dish.
13. Lift-off PS nanospheres with water sonication in a Branson ultrasonic bath for 30–60 sec to create origami binding sites. In the absence of an ultrasonic bath, continuous stirring in water for a longer period of time is adequate. The nanospheres visibly come off the surface.
14. Blow dry with a nitrogen "gun".
15. Bake at 120 °C for 5 min to stabilize the HMDS on the surface.

Note If you find areas without patterned DNA origami or binding sites, you may need a higher concentration of nanospheres (this is generally observed for 700–1000 nm nanospheres). A good sanity check is to label the origami with fluorophores, if possible, and observe under a fluorescence microscope for grids. AFM can sample a small fraction of a chip surface. For <500 nm nanosphere sizes, finding origami grids should not be a problem.

Origami placement experiments.

1. Thermal Cycler (Life Technologies) for origami annealing.
2. 100 kDa spin filter columns (Amicon).
3. A benchtop centrifuge (Denville, 6000 g, 3–5 rounds of 5–min spin) for origami purification.
4. Origami: Modified circle with a square hole *aka* Death Star.[59]
5. Tris-HCl buffer (Buffer 1: pH 8.35, 40 mM Mg^{2+}, 40 mM Tris, and Buffer 2: pH 8.9, 35 mM Mg^{2+}, 10 mM Tris) [Magnesium Chloride Hexahydrate | M9272-500G, Sigma; Tris, T-400-1 GoldBio].
6. 50%, 75%, and 85% Ethanol (459836 Sigma Aldrich) in ultrapure water.

A step-by-step protocol for origami placement and washing steps.

1. Incubate chips with ∼100–200 pM origami (nominal concentration for 1 μm pitch, concentration inversely proportional to nanosphere size) in ∼ 40 mM Mg, Tris-HCl (40 mM Tris) buffer (pH- 8.3) for 60 min.
2. Wash in ∼ 40 mM Mg, Tris-HCl (40 mM Tris) buffer (pH- 8.3) for 5 min either manually or automatically using a peristaltic pump or shaker in a petri dish.
3. Transfer to ∼40 mM Mg, Tris-HCl (40 mM Tris) buffer (pH-8.3) + 0.07% Tween 20 and wash for 5 min.
4. Transfer to ∼35 mM Mg, 10 mM Tris (pH-8.9) to hydrolyze HMDS and lift off origami non-specifically bound to the background, and wash for 5 min.
5. For AFM characterization, transfer to ethanol drying series: 10 seconds in 50% ethanol, 20 seconds in 75% ethanol, and 2 min in 85% ethanol.
6. Air-dry, followed by AFM/fluorescence verification of patterning.

Note All of the work reported in this paper was performed with spin-column purified origami, which is suitable for small amounts of origami. After purification and quantification, it is critical to use DNA LoBind tubes (Eppendorf) for storage and dilution of low concentration DNA origami solutions. Low dilutions, *e.g.* 100 pM, must be made fresh from more concentrated solutions and used immediately—even overnight storage can result in total loss of origami to the sides of the tube. Addition of significant amounts of carrier DNA to prevent origami loss may prevent origami placement, just as excess staples do. We have not yet determined whether other blocking agents such as BSA might prevent both origami loss and preserve placement.

S3. AFM characterization

All AFM images were acquired using a Dimension FastScan Bio (Bruker) using the "short and fat" or "long and thin" ScanAsyst-IN AIR or ScanAsyst-FLUID+ cantilever ("sharp nitride lever"(SNL), 2 nm tip radius, Bruker) in ScanAsyst Air or Fluid mode. All samples were ethanol dried prior to imaging. Single and multiple binding events for placed origami were hand-annotated for origami occupancy statistics and image averaging of arrays (imageJ) was used to determine binding site size. The mean spacing between neighboring binding sites in (**Fig. 3M**) was measured from the FFTs of the corresponding AFM images (**Fig. 3G–L**) using imageJ.

S4. SEM characterization

Images of close-packed nanosphere crystals, as well as individual nanosphere cross-sections, were obtained using a Hitachi S-4700 Field Emission Scanning Electron Microscope (ASU Nanofab, Center for Solid State Electronics Research, Tempe, AZ) at 1–5 keV, and the stage (or electron beam) was manipulated as required. In order to prevent charging effects and distortion of the image collected, a sputter coater (Denton Vacuum Desk II, New Jersey) was used to coat the specimen (glass with nanospheres) with Gold-Palladium (Au-Pd), and carbon tape was used to provide a conduction path from the glass surface to the SEM stub (ground). For the cross-sectional images specifically, the glass coverslip was broken in half post sputter-coating and

wedged inside a standard cross-sectional SEM sample holder such that the electron beam impinged directly on the flat edge of the glass coverslip to visualize the contact areas between the nanospheres and the glass surface. Measurements from high-resolution images were made manually using imageJ.

AFM *vs.* SEM analysis of binding site size. Over the range of nanosphere diameters tested, we found a global discrepancy of $\sim$11% between the linear fits, with SEM ($a = 0.38 d_{ns}$; **Fig. 3A–F**) providing consistently larger estimates than AFM ($a = 0.27 d_{ns}$; **Fig. 3G–L** and **N**). We first note that each of the SEM mean and SD values are gleaned from $N = \leq 10$ nanospheres, whereas corresponding AFM values are determined using weighted means and SDs from averaged images of $N > 400$ binding sites for any given nanosphere diameter.

We offer two possible explanations for the observed discrepancy:

(*i*) HMDS is a miniscule molecule which can lead to larger coverage of interstitial spaces between nanospheres than can be accurately measured using an indirect technique, such as SEM. This may result in overestimation of masking areas when examining electron micrographs. In addition, all SEM images were collected by sputter coating sample cross-sections with a $\sim$10-nm Gold-Palladium (AuPd) layer (for conductivity), which may further contribute to higher estimated values. AFM, however, provides a direct mode of measurement post-passivation with HMDS, and can facilitate a more precise estimation of the "footprint" of each individual nanosphere in an HCP layer.

(*ii*) On closer observation of electron micrographs, we found an apparent distortion of nanosphere geometry along the xy-axes in keeping with the phenomenon of Hertzian contact (**Fig. 3A–F**). This alteration in morphology could be linked to the position of each nanosphere, and/or the electron beam with respect to the substrate edge, as well as the relative position of each nanosphere to other, adjacent spheres, and the physical contact between individual nanospheres and the glass surface. It is plausible that attractive forces during the solvent evaporation process contribute to the departure from a spherical to a more flattened shape upon interaction with neighboring colloidal particles. Using a simplistic deformation model to support this hypothesis (**Fig. S3**), we note that for an 8% distortion along the vertical axis of a nanosphere (80 nm for a 1 μm diameter), the predicted binding site size follows the experimental SEM values closely. This may help explain the discrepancy between the observed SEM and AFM values in a quantitative manner, with SEM images overestimating the effect of distortion caused by physical deformation on binding site sizes obtained.

S5. DNA–PAINT

All TIRF experiments were conducted on a benchtop super-resolution Oxford Nanoimager (Oxford, UK). For control DNA–PAINT experiments, a glass chip was activated for 10 min, followed by the creation of a "flow chamber" (using double sticky Kapton polyimide adhesive tape; Amazon) and 30–min incubation of 400 pM DNA origami at 40 mM Mg^{2+}. Non-specifically bound origami were washed off using several rounds of wicking the incubation buffer through the chamber. Next, a 0.05% Tween–20 (Cat no. P1379, Sigma Aldrich) v/v in 40 mM Mg^{2+} placement buffer was flown through several times before incubating the solution for 5 min. This prevents non-specific *ss*DNA binding during the experiment (**Fig. 5E** and **G**). Subsequent washing in Tween–buffer, and placement buffer was followed by the introduction of up to 5 nM P1-imager solution in placement-Tween buffer, 10x dilution of 40-nm Gold nanoparticles (fiducials for drift correction, Sigma Aldrich 741981), and an oxygen scavenging system (2x, 3x, 5x concentrations of PCA, PCD, and Trolox-Quinone, respectively). To ensure the gold nanoparticles settle on the bottom chip, it was taped to a 96-well plate holder in a centrifuge and spun at 150 g for 5 min, ensuring that the inlet and outlet of the flow chamber were sealed prior to spinning. Experiments with patterned chips were conducted by sticking the 10×10 mm^2 coverslip onto a double-sided sticky Kapton tape, and repeating the procedure as outlined above starting with incubation with 0.05% Tween–20 in placement buffer.

DNA–PAINT data were analyzed using Picasso.[11] Briefly, a dataset <4 GB was prepared for analysis on Picasso ["`Localize`"]. A minimum net gradient of 5,000 was chosen to avoid non-specific signals from

being analyzed. After the fits were found, the `.hdf5` file was loaded into the Filter module of Picasso. This module allows localization precision filtering, as well as the filtering of "double" localizations, by manually selecting a Gaussian profile of localization photons. The filtered localizations dataset is then loaded into Picaso `Render` where multiple cross-correlation-based drift corrections and multiple corrections based on picking fiducial markers on the sample 40-nm gold beads and/or origami themselves ["`pick similar`"]) were used to perform more precise drift correction. The threshold was adjusted prior to automatic or manual picking of structures to be averaged. The picked localizations were then registered into Picasso `Average` where they were aligned using center of mass followed by multiple iterations of rotational and refined translational alignment to form the final "summed" image. A nominal oversampling value of 200 was used to represent the structures prior to measuring the PSFs in imageJ using an ROI drawn around each vertex and finding its full width at half maximum (FWHM; **Fig. 5K–M**).

Buffer components	**Volume (μL)**
Imager "P1" strand in 40 mM Mg^{2+} + 0.05% Tween–20 (10 nM, stock)	30
40 mM Mg^{2+} + 0.05% Tween–20	16.7
40 nm gold nanoparticles	6
50× PCA	2.5
100× PCD	1.8
100× Trolox–Quinone	3
Total	60

Table S1. Buffer composition of DNA–PAINT experiments.

Note

1. A concentration beyond 0.1% Tween–20 may result in disassociation of origami from the binding sites.
2. All datasets analyzed had duty cycles of 1:10–1:50 (10,000–12,000 frames), and were screened based on amount of photobleaching as a quality-control measure.

S6. Photobleaching experiments

For the photobleaching experiments, we analyzed the intensity traces of origami molecules in response to laser excitation and observed steps corresponding to independent, stochastic fluorophore quenching events. Based on a histogram of the number of fluorophores experimentally found to be incorporated per origami baseplate we calculated the strand conjugation efficiency to be 56%. For these experiments we assumed that the fluorophore-of-interest was indeed conjugated to the strand complementary to the six handle strands, and that it was not photobleached prior to experimental observation. Yields of 84% have been previously reported,[13] and we hypothesized our observation of lower yield could possibly be due to poor strand accessibility. It is important to note that the circular origami have been experimentally shown to break up-down symmetry using staples modified with 20`T` extensions that act as entropic brushes, with 95.6% origami facing the designed-side up.[59] While this is experimentally advantageous in terms of number of structures facing right side up, and consequently the amount of useful data collected, it is plausible that these 20`T` extensions may result in steric hindrances and poor accessibility of the strands-of-interest. We tested several conditions such as circumventing the dehydration step (to rule out the accessibility problem), increasing strand-excess, increasing annealing time, and additionally, directly annealing the fluorophore-labeled complementary strands with the handle strands. We did not find any significant changes in incorporation efficiency with yields of ∼60% in all cases. Based on these observations, we posit that the sub-par conjugation efficiency may be sequence-, strand concentration-, strand purity-, strand position on origami-, or origami purification strategy-dependent. This low yield, while concerning, is a broader concern for the field of structural DNA nanotechnology itself and a comprehensive examination may require a more

concerted effort by the community.

Photobleaching experiments were performed immediately after grid formation in imaging buffer (1x TAE. 12.5 mM Mg^{2+}) and oxygen scavenging similar to DNA-PAINT). Control experiments of randomly immobilized origami were also performed. There was no difference in the conjugation efficiency with and without patterning. Similarly, no difference was observed when origami were pre-labeled (*i.e.* P1P4-Cy3B strand annealed with origami in a one-pot reaction) in comparison to being post-labeled once on the surface of the chip. In both cases, fluorophore-labeled strands were added at a concentration between 10–100 nM (*i.e.* 10–100x excess). Laser intensity was adjusted in order to have a slow gradient of fluorophore intensity bleaching to make step-counting easier. Steps were quantified using two methods: imageJ,[63] and iSMS[64] (http://inano.au.dk/about/research-groups/single-molecule-biophotonics-group-victoria-birkedal/software/). For the latter, the field-of-view was cropped, and the two ROIs were aligned to distinctly count the number of steps.

The following were the criteria when analyzing photobleaching data:

1. Must bleach completely.
2. Must have the signal of a single molecule, and not aggregates.
3. Must show ≤ 6 photobleaching steps.
4. Must have a consistent step size.

S7. Guide to troubleshooting binding site creation and origami placement

Problem	Likely cause(s)	Potential solution(s)
Nanosphere pellet is absent	1. Spin speed is too low to sediment beads out of solution.	1. Spin speed/time required for pellet formation is inversely proportional to nanosphere size and should be adjusted accordingly. 2. Use a different rotor.
Nanospheres do not adhere to the glass surface.	1. Improper plasma activation.	1. Contact angle measurements should delineate the difference between "inactive" and "active" glass surfaces.
	2. Improper ethanol concentration.	2. Start at a nominal, 25% ethanol, but 50% should be give desired results. 3. Low nanosphere concentration.
No nanosphere close-packing observed.	1. Traces of surfactant in the original solution prevents self-assembly of nanospheres.	1. Wash $\geq$2 times and resuspend in pure water before preparing a final suspension in 25% ethanol at the appropriate nanosphere concentration.
	2. Final ethanol suspension might have surfactant due to incomplete wash steps.	2. Carefully aspirate supernatant from the end opposite to the pellet on the Eppendorf tube.
Nanospheres do not come off after sonication.	1. Sonication intensity may be low.	1. Use an 80×40 mm^2 Pyrex petri dish (3140; Cole-Parmer) for sonication and leave the dish in the bath for *geq*5 mins if necessary
Alternative: Chips can be inserted in a petri dish containing an organic solvent such as Tetrahydrofuran (THF, 401757, Sigma) heated to 60 °C for 5–15 mins to dissolve beads. Care must be taken when handling THF, and to reduce evaporation owing to its volatility.	2. Dehydration bake temperature may be too high.	2. The glass transition temperature (T_g) of polystyrene nanospheres is ∼80 °C and should not be exceeded to prevent nanospheres from losing their integrity.

Binding site variability is observed over the surface of the chip.	1. Insufficient dehydration baking time results in "water puddles" around the nanosphere "footprints" preventing HMDS from depositing all around the circumference.	1. Increase initial dehydration bake time to 10 min.
	2. Nanospheres are not NIST-standards approved, *i.e.* large standard deviation in nanosphere size.	2. (*i*) Check with the manufacturer to confirm SD from the nominal size of nanospheres. (*ii*) Measure the distribution of nanosphere size.
Binding sites are hard to find using AFM.	1. AFM tapping force under threshold value.	1. Tune scanning parameters to rationally to image binding sites.
	2. Scanned area is devoid of nanosphere close-packing.	2. Proceed to origami placement to simplify AFM imaging. Origami nanostructures provide better contrast.
		3. Sample at least one area from each quadrant of the chip to determine the source of the issue conclusively.
Impurities on the surface	1. Improper cleaning	1. More aggressive cleaning required (*e.g.* RCA).
	2. Dirty plasma chamber.	2. Clean plasma cleaner chamber with isopropanol, let dry, run it without a sample for an hour, clean again (checking for contaminant residues after every step).
	3. Failure to perform "descum" plasma step, which can leave the particulate matter in the interstitial spaces.	3. Filter all buffers used during wash steps.
		4. Ensure petri dishes are clean.
		5. If using automated washing, always sterilize peristaltic pump tubing by running boiling hot water through it first, followed by a gradient of 100%, 75%, and 50% ethanol in pure water, and finally placement buffer just before use.
Origami bound non-specifically all over the surface.	1. Poor HMDS quality.	1. Dehydrate the wafer by baking before and after HMDS monolayer formation.
	2. Bake step for HMDS stabilization was accidentally skipped.	2. Keep pH<9, preferably at 8.3–8.5

	3. Improper washing and failure to remove weakly bound origami from HMDS background - new buffers may be required	3. Reduce Mg^{2+} concentration, and compensate by increasing origami concentration/incubation time 4. Keep incubation between 30–90 minutes 5. Remove weakly bound origami with more aggressive Tween-20 washes (0.08%, 10-20 minutes). 6. Remove any hydrophobic moeties (*e.g.* fluorophore) from the origami. Note that HMDS is hydrophobic.
Low DNA origami occupancy.	1. Old chip with inactive sites.	1. Sites remain optimally active for $\lesssim$4 hours post-plasma cleaning.
	2. Low origami concentration.	2. Always optimize origami concentration (*e.g.* 4 chips, 200–400 pM for 400-nm spacing). Use higher origami concentration, prepare fresh dilutions, and use immediately
	3. Short incubation time	3. Check buffer pH (8.3–8.5), prepare fresh if necessary, with 35 mM Mg^{2+}.
	4. Low pH, or Mg concentration.	4. Add a verification step to ascertain appropriate binding site diameter post nanosphere lift-off using AFM.
High multiple DNA origami occupancy.	1. High origami concentration.	1. Optimize origami concentration every time fresh stock is prepared.
	2. Long incubation time.	2. Use an incubation time between 30–90 minutes
	3. Oversized feature	3. Add a verification step to ascertain appropriate binding site diameter post nanosphere lift-off using AFM 4. Check buffer conditions

High background binding: Origami (balled-up [white "blobs"] or otherwise)	If HMDS passivation is good, origami cannot bind flush against the surface, and improper washing can lead origami to come off partially. Subsequent ethanol washing leads to any origami not bound completely to ball up and appear as white blobs during AFM imaging.	1. Dehydrate the chip before and after HMDS monolayer formation taking care to keep first dehydration step below T_g of polystyrene nanospheres 2. Keep placement buffer pH between 8.3–8.5 3. Remove weakly bound origami with longer Tween-20 wash and/or increasing Tween-20 concentration (<0.1% to prevent origami in binding sites from falling off).
Origami fall off during ethanol drying.	Too much time spent in dilute ethanol (<80%).	Move quickly from low to high % ethanol.
Origami ball up into site during ethanol drying and corners are double height.	Origami project partially onto non-sticky HMDS surface.	Hydrolyze HMDS surface before drying by washing in pH 8.9–9.0 buffer to mitigate background binding.
Binding sites are filled up, but no defined origami shapes observed	Excess of staple strands.	1. Check scaffold and origami integrity using gel electrophoresis and AFM pre and post-purification 2. Scaffold quality might be a problem

S8. Supplementary Figures

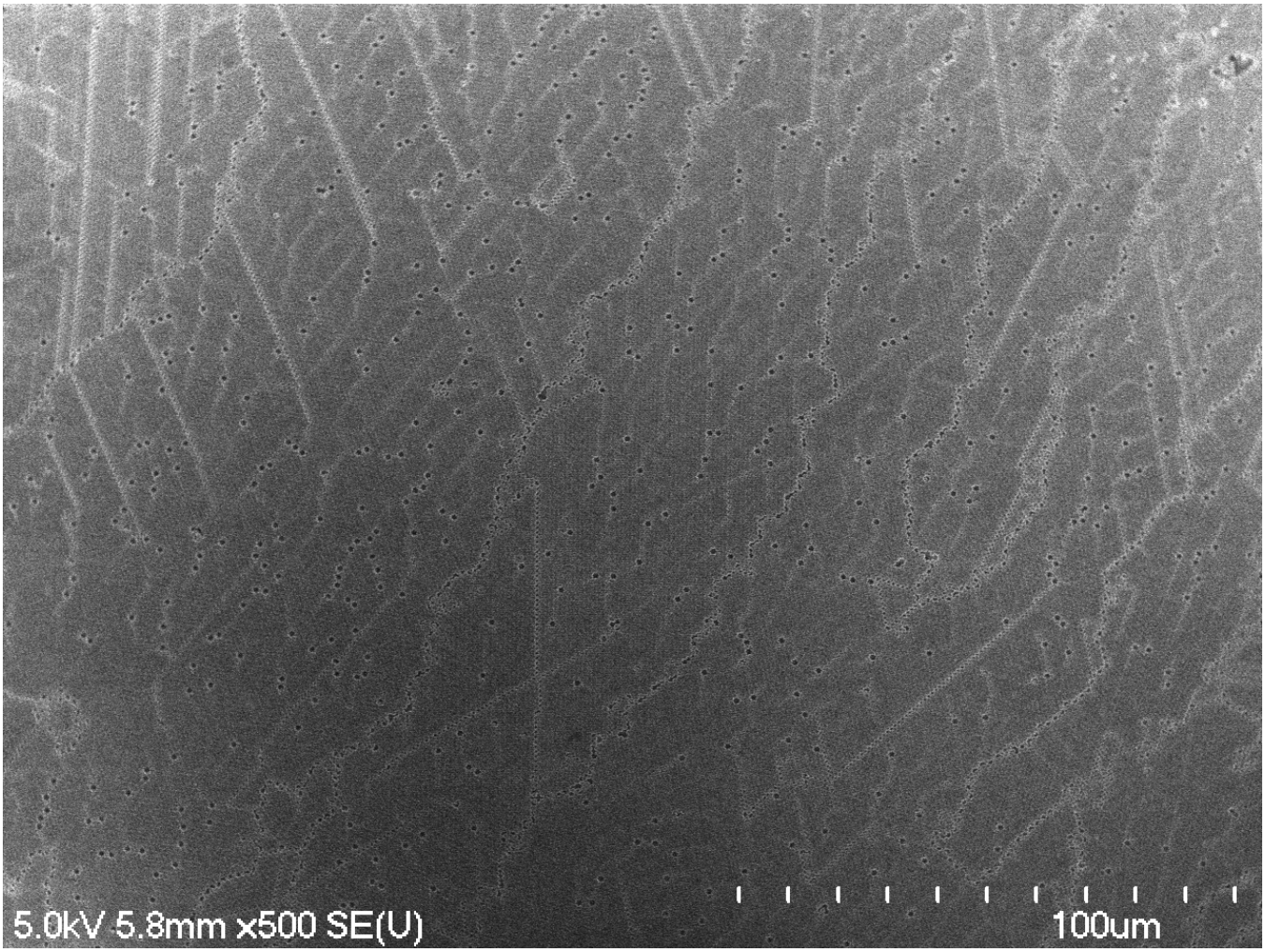

Fig. S1. An SEM image of a monolayer of nanospheres exhibiting close-packing and long-range crystallization at the mesoscale.

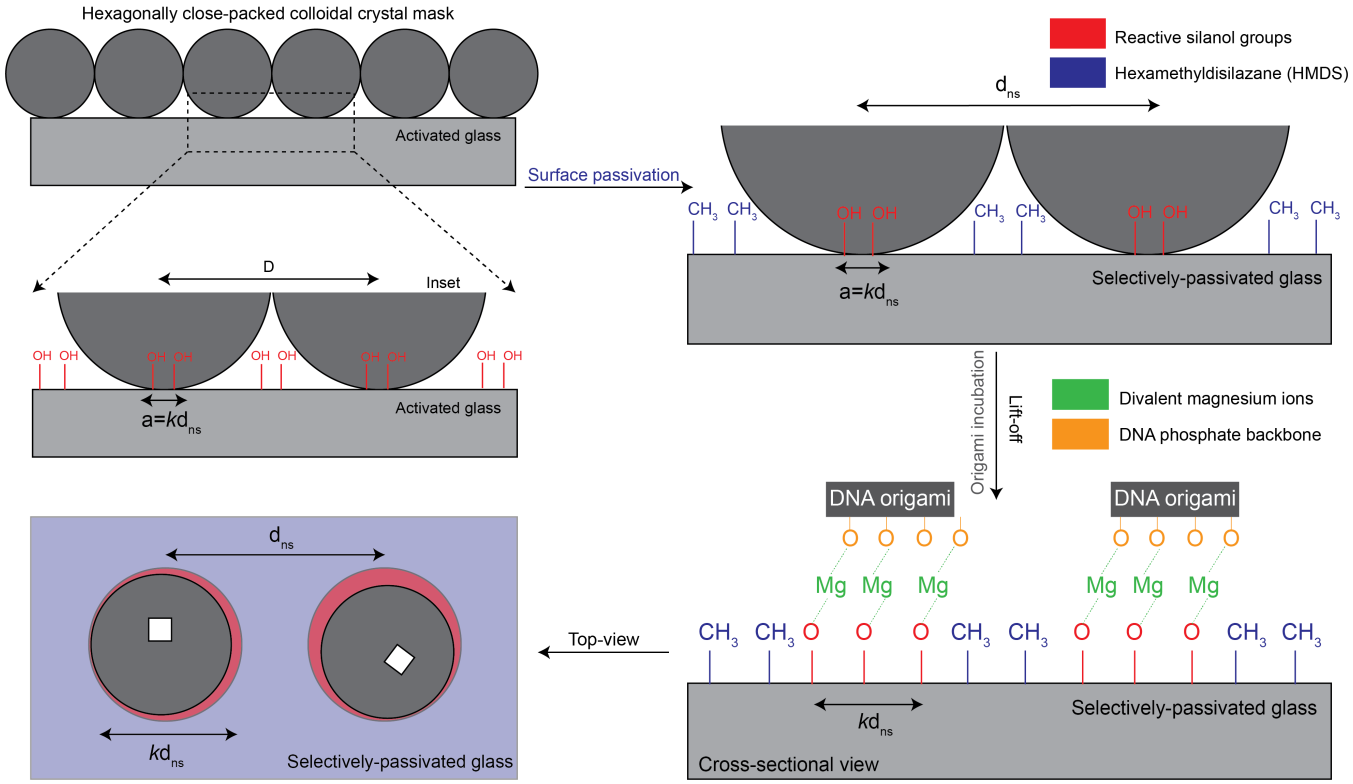

Fig. S2. Schema of reactive silanol groups being protected by a colloidal crystal mask (CCM) of appropriately sized nanospheres. Each nanosphere footprint is intrinsically linked to its diameter a by the relation: $a = kd_{ns}$. A bulk surface passivation step with HMDS results in the selective passivation of the entire chip surface with neutral and hydrophobic methyl groups. Upon lift-off of nanospheres, magnesium-mediated placement of negatively charged DNA origami to the reactive silanol groups formerly protected by the spheres proceeds through a process of diffusion, and alignment, prior to immobilization.[37] The important parameters that determine quality of nanoarray formation are Mg^{2+} concentration, pH, incubation time, origami concentration, and adequate washing (to reduce spurious background bindings).

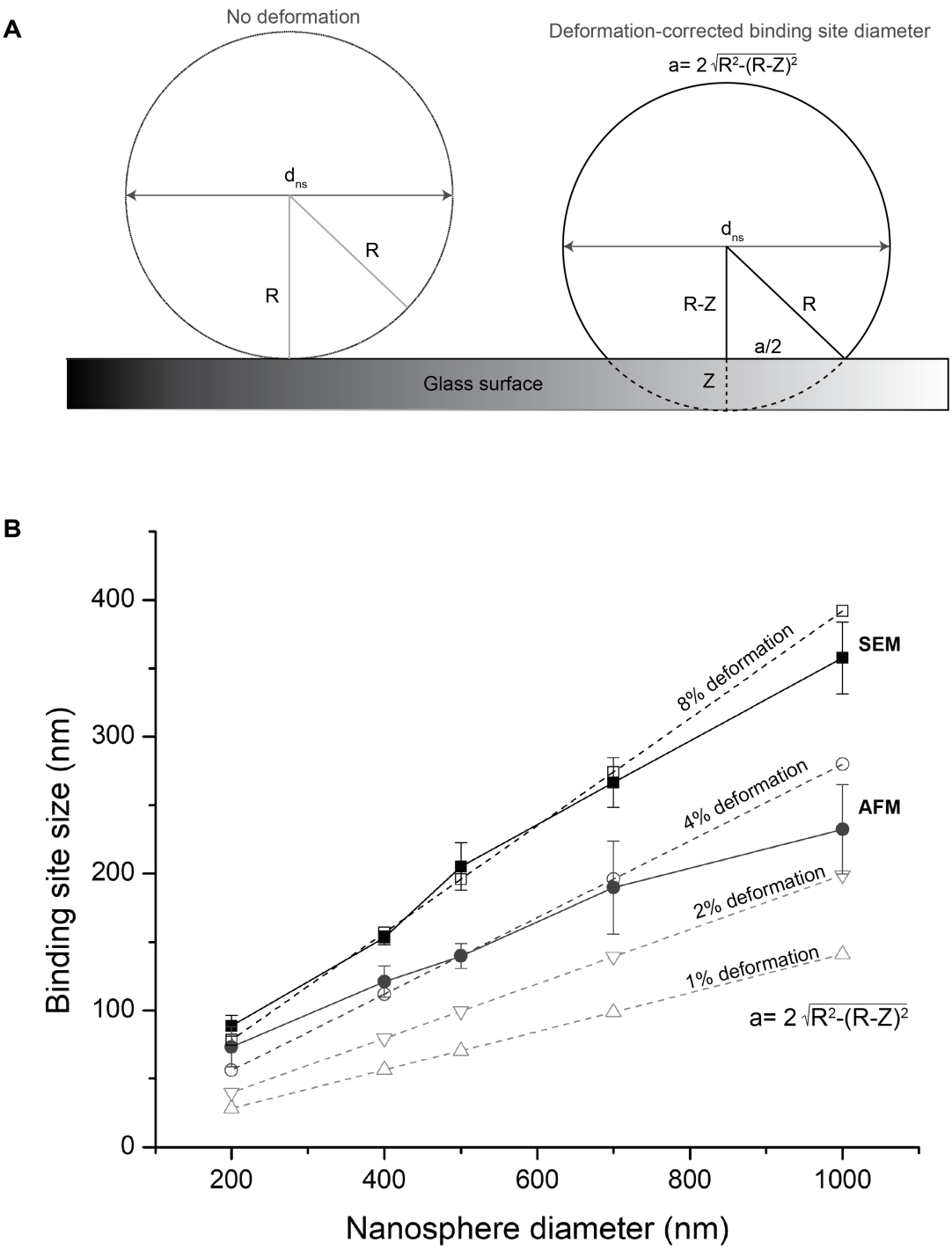

Fig. S3. EM images in **Fig. 3A–F** point to deformation of nanospheres resting on the surface due to Hertzian contact: interactions between adjacent spheres as a result of the capillary forces that drive them together during the process of close-packing, and interactions between the spheres and the surface. (**A**) The deformation-free case (left), and the distortion of nanosphere geometry owing to deformation (right), where a denotes the predicted binding site diameter owing to the deformation. (**B**) Plots the deformation-associated binding site diameters (for 1%, 2%, 4%, and 8% deformation) in comparison with binding sites measured *via* SEM (**Fig. 3A–F**) and AFM (**Fig. 3G–L**). Based on the relationship provided here, the co-efficient *k* in the relationship $a = kd_{ns}$ is 0.27 for AFM, and 0.38 for SEM, $i.e.$ the binding sites are expected to be 27% and 38% of their corresponding nanosphere diameters. As seen here, a deformation of 8% closely follows the values obtained using SEM measurements (indirect) which overestimate the binding site size compared to the 4% deformation predicted by AFM (direct) values, as alluded to in Supplementary Section **S5**.

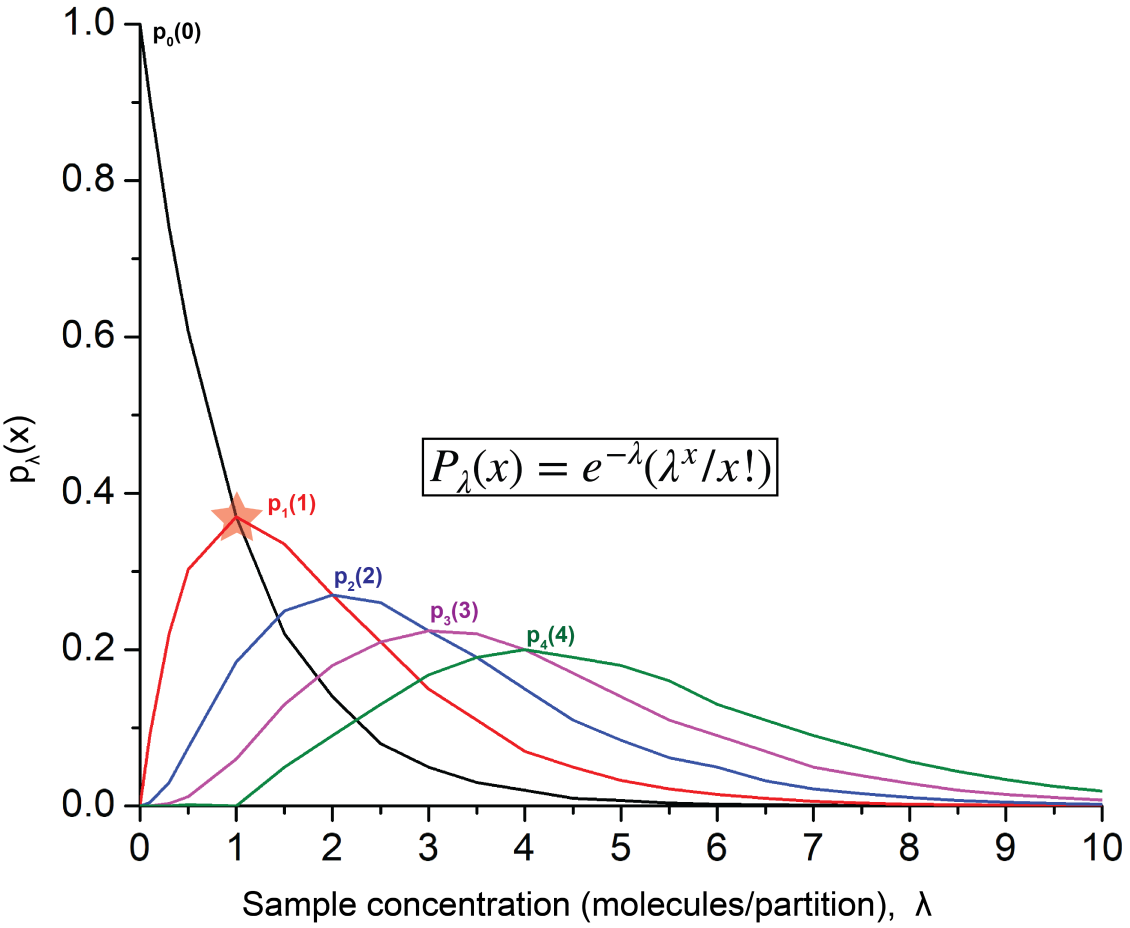

Fig. S4. The Poisson distribution which poses a statistical limitation on the probability of a single molecule occupying in each partition/well on a substrate. It quantifies the probability for finding 0, 1, or more than 1 molecule in a single partition (binding site in this study) given a certain sample concentration. The highest single molecule occupancy/binding efficiency occurs in the case where the ratio of molecules to wells is one and is maximally 37% (red star). This is the case for every stochastic top-down loading process unless a steric hindrance approach in the form of a DNA origami macromolecule (in this study) is used to prevent multiple molecules from binding to the same spot, consequently driving the single occupancy beyond the Poisson limit, as reported in (**Fig. 3O**; horizontal dashed line)

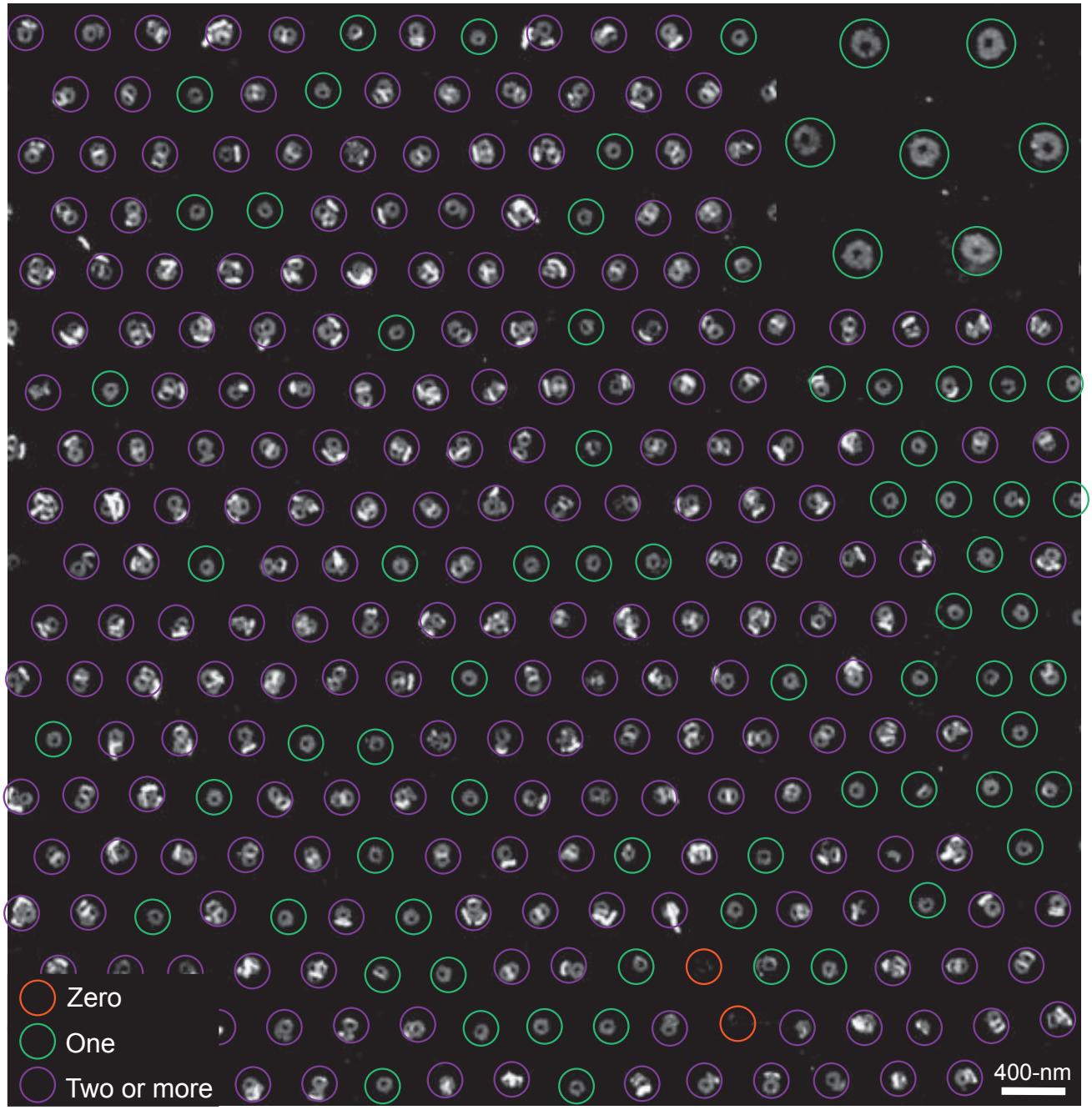

Fig. S5. A representative AFM image of a DNA origami nanoarray fabricated using 15 mM Mg^{2+} by varying other governing global parameters, such as origami concentration, incubation time, and buffer pH. Experimental parameters here were 250 pM origami, 90–min incubation, and pH = 7.8. Zero, one, and two or more indicate number of origami occupying a binding site.

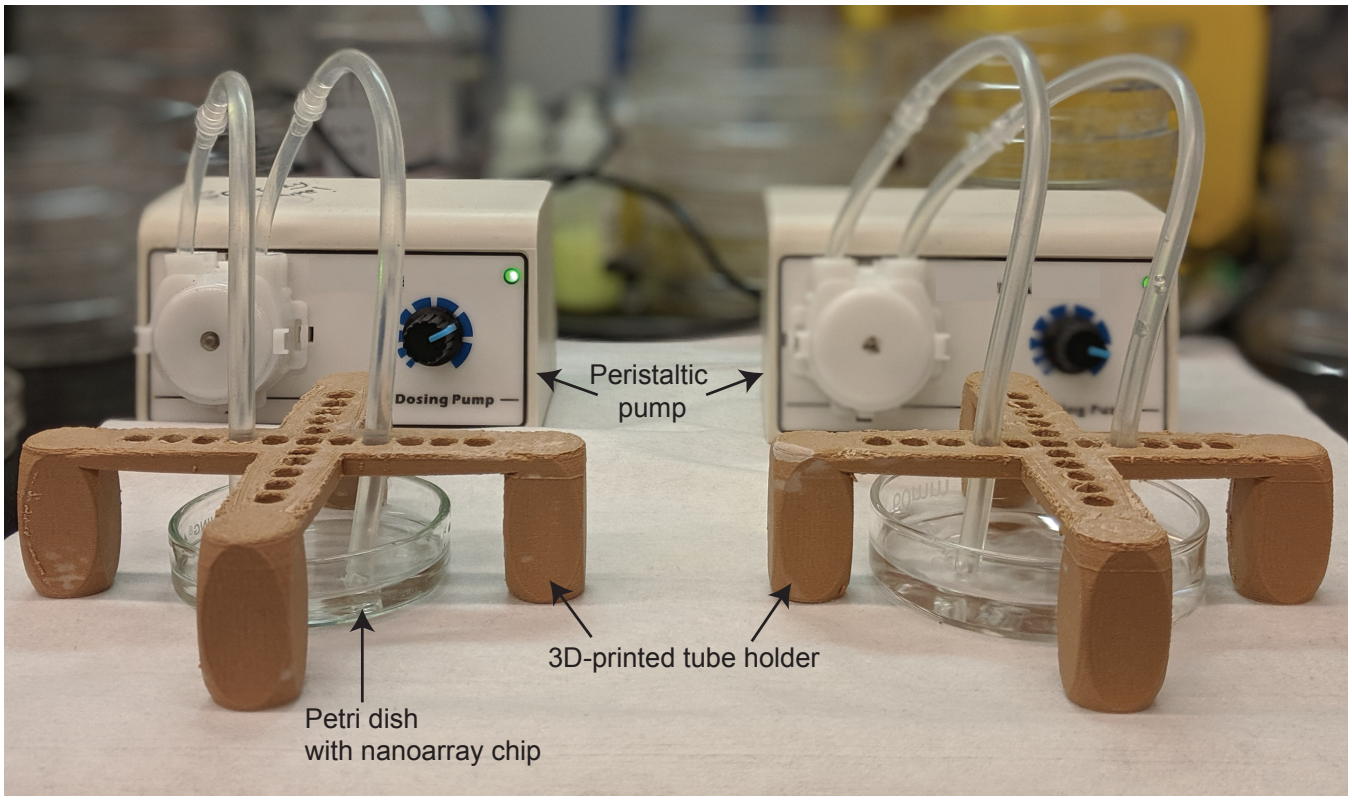

Fig. S6. Peristaltic pumps for automating the three 5–min wash steps for optimized cleaning of nanoarray chips. We use 3D-printed tubing holders to maintain a constant position for consistency in quality. The peristaltic pumps primarily mitigate user-variability introduced during the wash steps. Alternatively, a rocker with parameters adjusted for optimal washing can be used for consistent automated wash steps.

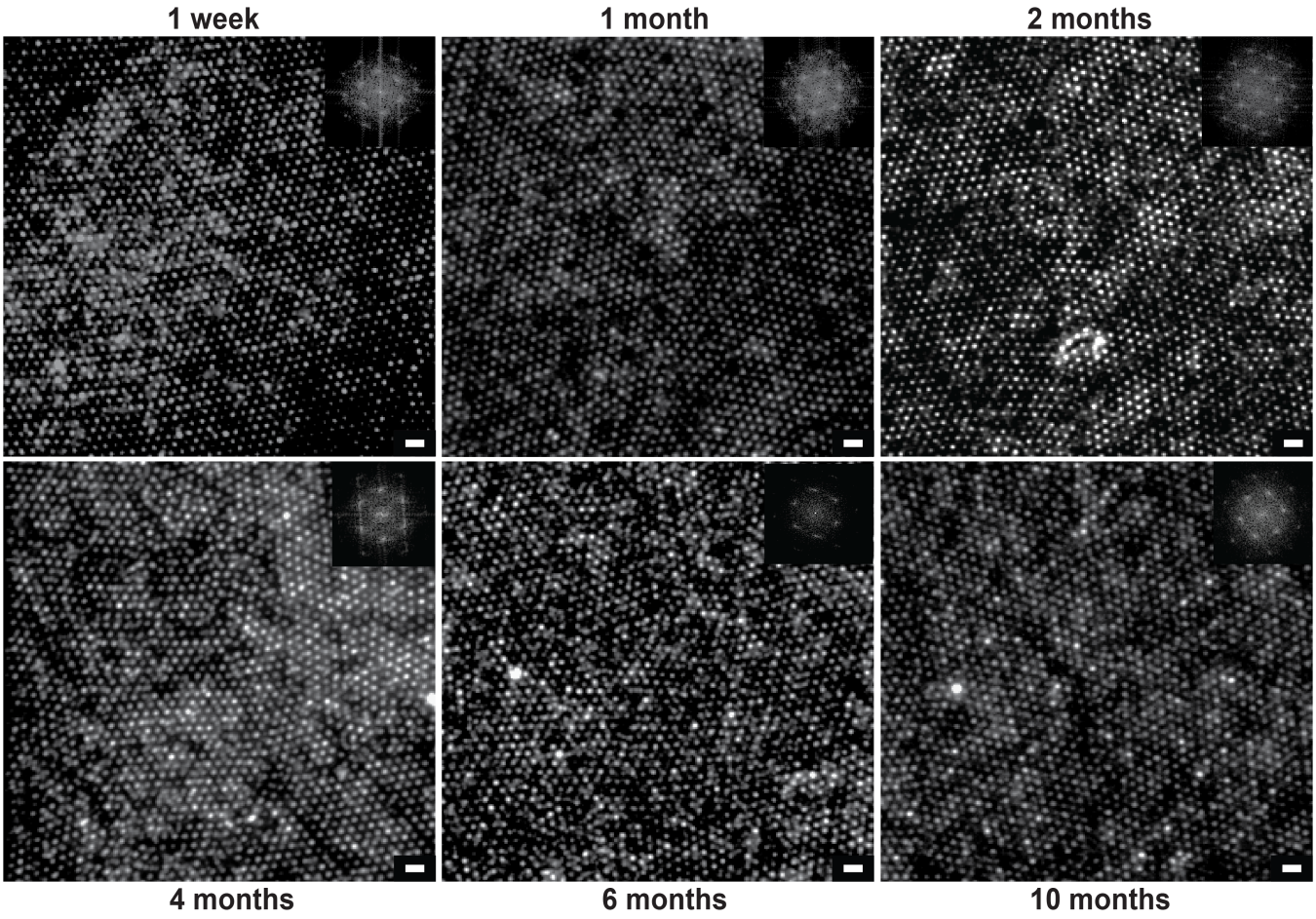

Fig. S7. The functional viability as well as the quality of stored DNA origami nanoarrays over several months. Fluorescence images of DNA arrays after indicated storage time. DNA nanoarray shelf-life was validated using two chips for each time point: one labeled with fluorophores, and the other unlabeled. The chips were covered in aluminum foil and stored in a drawer at room temperature for up to 10 months. At each time point until 2-months, both chips were visualized with the second being labeled immediately prior to observation in 1x TAE, 12.5 mM Mg^{2+}, 0.05% Tween–20. Post 2-months, already labeled chips were visualized every month for quality assessment. Insets: 2-D FFTs of each micrograph. Scale bars are 1 μm.

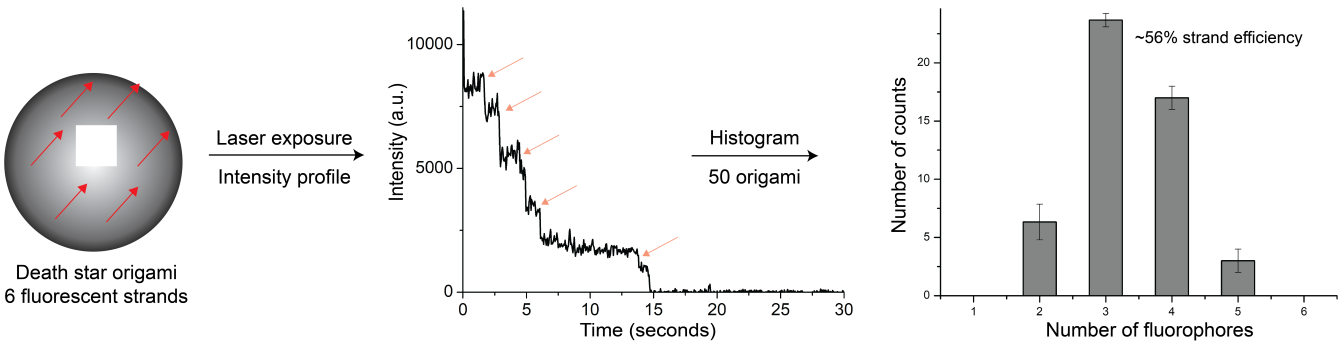

Fig. S8. Conjugation efficiency of fluorophore-labeled strands of DNA origami nanoarray samples. (Left) Six 20-nt sequences (same locations as PAINT docking sequences), detailed in **Table S1**, hybridize complementary, fluorophore-labeled strands ($\leq$10x excess) for 30 min in 1x TAE, 12.5 mM Mg^{2+}, 0.05% Tween–20. (Middle) The fluorophores were photobleached over several min in the imaging buffer until all puncta disappeared. The intensity profiles of each DNA origami molecule were analyzed and the number of steps, corresponding directly to the number of strands conjugated to the origami baseplate, were counted using imageJ and iSMS. (Right) Finally, these steps were converted into a histogram to quantify strand incorporation/accessibility. For hexagonal vertices spaced 45-nm from each other, the strand conjugation efficiency is $\sim$56%, $i.e.$ 3.36 strands of a possible 6 ($N \geq$50).

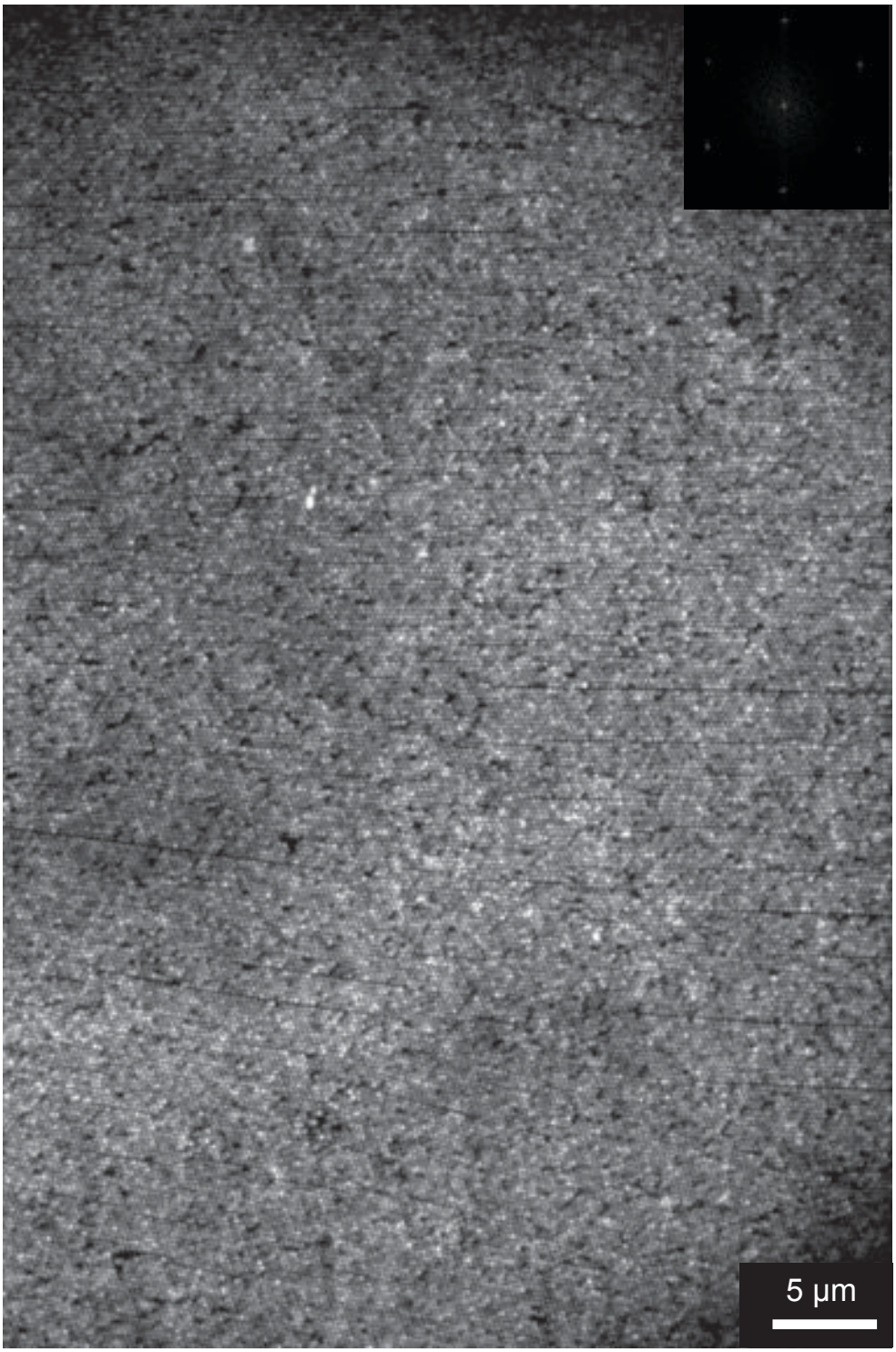

Fig. S9. A fluorescence image of 11,000 frames collapsed along the z-axis of a patterned PAINT dataset prior to drift-correction and data analysis on Picasso.[11] DNA origami nanostructures were placed on a grid of binding sites created by 350 nm nanospheres. (Inset) The FFT spectrum of the image confirms the hexagonal arrangement of DNA origami.

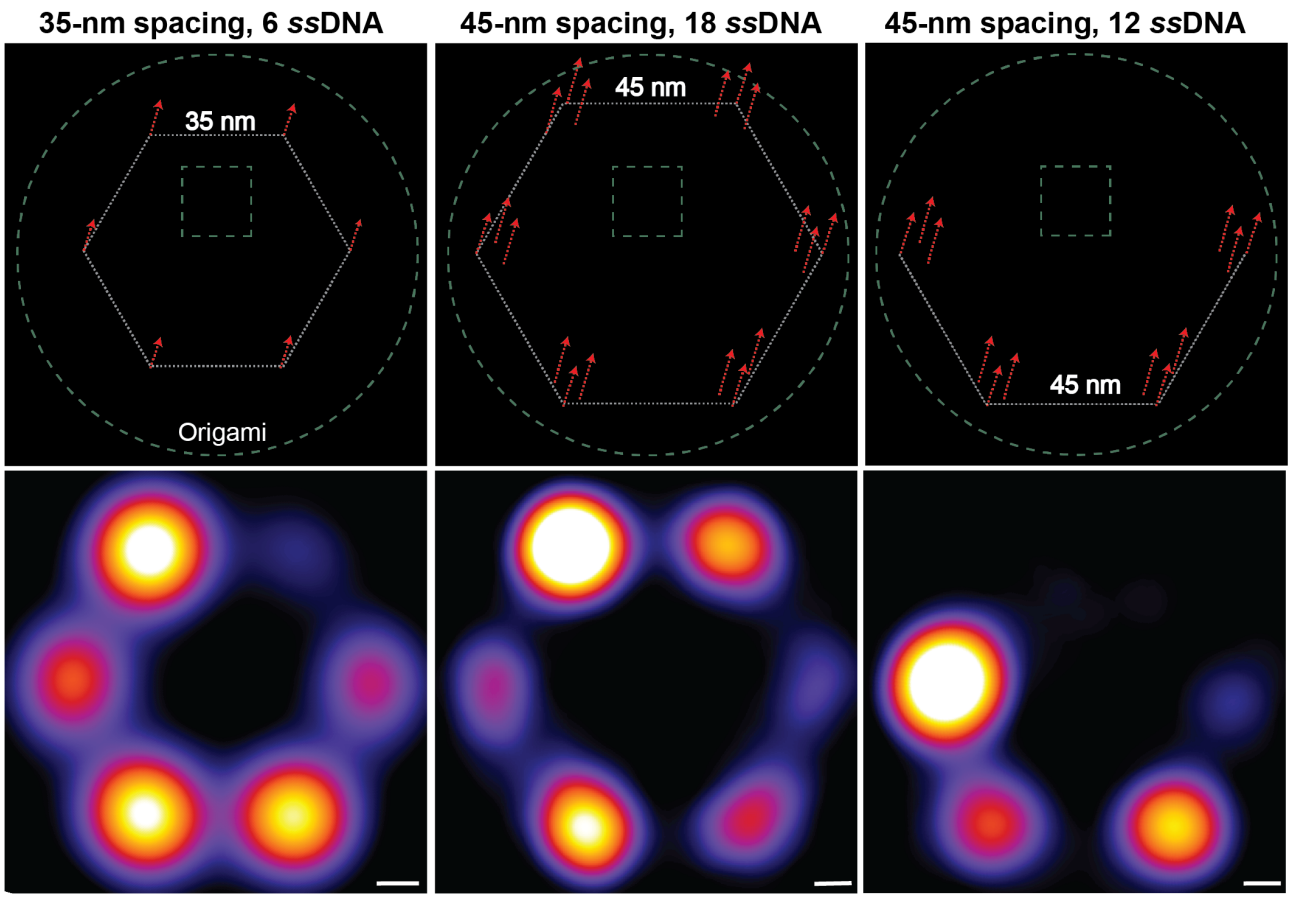

Fig. S10. Three configurations of DNA–PAINT experiments with indicated spacings as well as number of "docking" strands (6, 18, and 12), and their corresponding averaged images formed using 10 iterations at an oversampling of 200 on Picasso.[11] From left-to-right: Manually picked structures in Picasso from a patterned sample (N=300); and two randomly-immobilized samples (control; N=200 (middle); N=100 (right)). Each picked structure consists of at least 4 out of 6 vertices for the 6 (left) and 18 (center)-vertices samples, and at least 3 out of 4 vertices for the 12 (right) vertices sample. The last two columns use redundancies of docking strands to compensate for the 56% strand conjugation efficiency (**Fig. S8**). The first column combines a larger number of structures owing to the high-density of data available in experiments with DNA origami nanoarray patterning.

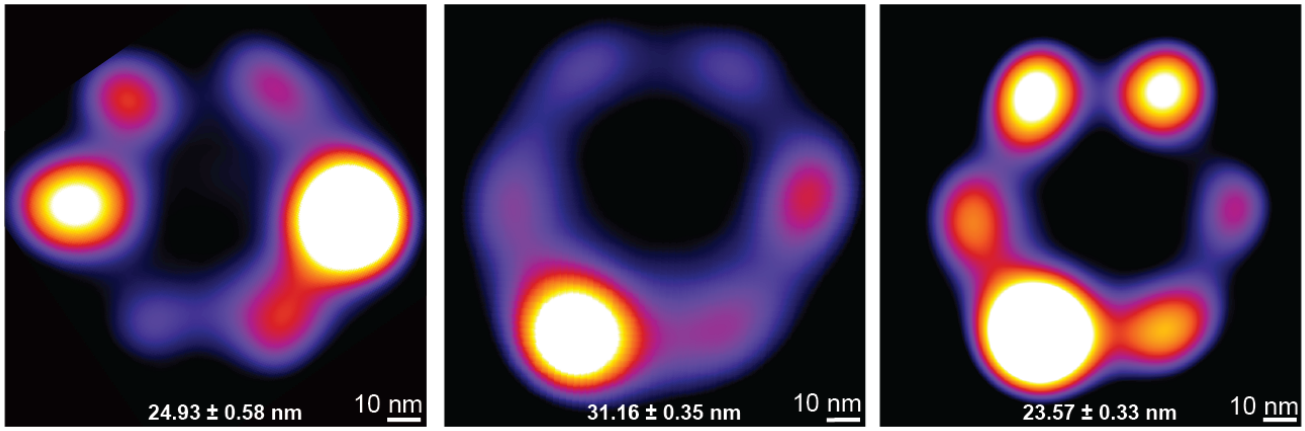

Fig. S11. An "averaged" image of automatically-picked structures corresponding to the low (100 pM, left), high (500 pM, center), and patterned (400 pM, right) experimental designs (left-to-right, N = 1800, 8000, and 5200, respectively). FWHM error expressed as SEM (**Fig. 5**). The data quality in the patterned case is similar to the case with low concentration, indicating that the overlapping of multiple structures in the high concentration case might lead to "false positive" particle picking and averaging by the automated program process flow in Picasso.[11] Notably, the theoretical improvement in throughput from the low concentration case to the patterned case is $\geq$10x.

S9. Supplementary Tables

Experiment	Description	Sequence
Photobleaching	P1 (9-nt) *P4*	/5AmMC6/ GTAGATTGATTAGATGTAT
	P1P4-A12-H3base128	ATACATCTAGATCAATCTACTTTTCGGAACGGCACCAACCTAAAACGGCGACCTG
	P1P4-B4-H3base256	ATACATCTAGATCAATCTACTTTTCAAGCCCAGGCGGATAAGTGCCGCCTGCCT
	P1P4-H7-H14base303	ATACATCTAGATCAATCTACTTTTAATGAAAGCCCAATAATAAGAGTAAGCAGA
	P1P4-H10-H14base79	ATACATCTAGATCAATCTACTTTTCATTTTGCAACTAAAGTACGGAGAGTACC
	P1P4-G11-H25base128	ATACATCTAGATCAATCTACTTTTCGCACTTACACTGGTGTGTTCCGTTTTCA
	P1P4-H3-H25base256	ATACATCTAGATCAATCTACTTTTAAATCCTTTGGCAAATCAACAGTCGGTCAG
PAINT (45-nm, 6 primary vertices)	P1(10-nt) *	CTAGATGTAT/3AmMO/
	9-nt P1 docking site	ATACATCTATTTT-Strand
	G11-H25base128-HCR-PAINT-large-P1P4-10mer	ATACATCTAGATCAATCTACTTTTCGCACTTACACTGGTGTGTTCCGTTTTCA
	H3-H25base256-HCR-PAINT-large-P1P4-10mer	ATACATCTAGATCAATCTACTTTTAAATCCTTTGGCAAATCAACAGTCGGTCAG
	A12-H3base128-HCR-PAINT-large-P1P4-10mer	ATACATCTAGATCAATCTACTTTTCGGAACGGCACCAACCTAAAACGGCGACCTG
	B4-H3base256-HCR-PAINT-large-P1P4--10mer	ATACATCTAGATCAATCTACTTTTCAAGCCCAGGCGGATAAGTGCCGCCTGCCT
	H7-H14base303-HCR-PAINT-large-P1P4-10mer	ATACATCTAGATCAATCTACTTTTCAAGCCCAGGCGGATAAGTGCCGCCTGCCT
	H10-H14base79-HCR-PAINT-large-P1P4-10mer	ATACATCTAGATCAATCTACTTTTCATTTTGCAACTAAAGTACGGAGAGTACC
PAINT (45-nm, 12 secondary vertices)	B7-H4base143-PAINT-Large-P1P4-10mer-3P	ATACATCTAGATCAATCTACTTTTCTACGAAGAGGGTAGCAACGGCTACCACGCAT
	F5-H23base128- PAINT-Large-P1P4-10mer-3P	ATACATCTAGATCAATCTACTTTTAAAAAAAGAGCCTCCGGCCAGAGCGCAGGCGC
	B10-H4base239- PAINT-Large-P1P4-10mer-3P	ATACATCTAGATCAATCTACTTTTGTTGATATACCACCCTCATTTTCACAGTACAAACTACAAC
	F9-H23base256- PAINT-Large-P1P4-10mer-3P	ATACATCTAGATCAATCTACTTTTCGGGAGAATCCTGATTGTTTGGTCGTATT
	B12-H5base128- PAINT-Large-P1P4-10mer-3P	ATACATCTAGATCAATCTACTTTTCTCCATGTCATAGGCTGGCTGACCTAATTTCA
	G3-H24base143- PAINT-Large-P1P4-10mer-3P	ATACATCTAGATCAATCTACTTTTCGCTGGCCCGCACAGGCGGCCTTAGCCGCCA
	C4-H5base256- PAINT-Large-P1P4-10mer-3P	ATACATCTAGATCAATCTACTTTTATTTCGGACAGAATGGAAAGCGCACCACCC
	G6-H24base239- PAINT-Large-P1P4-10mer-3P	ATACATCTAGATCAATCTACTTTTCTGAATAATACAGTAACAGTACCGGAAACAG
	G11-H13base288- PAINT-Large-P1P4-10mer-3P	ATACATCTAGATCAATCTACTTTTGAGTTAAATAGCAGCCTTTACAGTCTTACCA
	H3-H13base96- PAINT-Large-P1P4-10mer-3P	ATACATCTAGATCAATCTACTTTTAGTTTCATGGTCAATAACCTGTTTGCTAAATC
	A1-H15base288- PAINT-Large-P1P4-10mer-3P	ATACATCTAGATCAATCTACTTTTACGCTAACGCTTATCCGGTATTCTTATCATTC
	A5-H15base96- PAINT-Large-P1P4-10mer-3P	ATACATCTAGATCAATCTACTTTTGGTTGTACAACCCTCATATATTTTAGATCTAC
PAINT (35-nm, 6 vertices)	H4-H14base111- PAINT-small-P1P4-10mer	ATACATCTAGATCAATCTACTTTTCGCAAATTCCATATAACAGTTGCCGGAAGC
	H6-H14base271-PAINT-small-P1P4-10mer	ATACATCTAGATCAATCTACTTTTACATAAAAATCAGAGAGATAACCCGAAACCGA
	E9-H22base143- PAINT-small-P1P4-10mer	ATACATCTAGATCAATCTACTTTTCGGGAACGGATTAAGTTGGGTAACGTGTAGAT
	E12-H22base239- PAINT-mall-P1P4-10mer	ATACATCTAGATCAATCTACTTTTACATAAATAAGACGCTGAGAAGAGGTTTGAA
	C9-H6base143-PAINT-small-P1P4-10mer	ATACATCTAGATCAATCTACTTTTACCAGGCGTACTTAGCCGGAACGATAATGCCA
	C12-H6base239- PAINT-small-P1P4-10mer	ATACATCTAGATCAATCTACTTTTAATTTACCTAAACAGTTAATGCCCTCGAGAGG
Origami labeling	PolyA-Cy3b	/5AmMC6/AAAAAAAAAAAAAAAAAAAA

Table S2. Modified strands for single-molecule experiments. The computer-aided design file, list of staples, and the staple map are included as a zip archive: `Origami designs+staples+movie.zip`.

Components	**Estimated cost/chip**
DNA origami	\$0.10
Nanospheres	\$0.50–1.00
Glass coverslip	∼\$0.50
Passivation layer	∼\$0.10
Total	**\$1.20–1.70**

Table S3. Conservative estimate of the cost of nanosphere lithography-based origami patterning materials and reagents.

	Probability of a binding site with		
Nanosphere diameter (nm)	**0** origami	**1** origami	≥**2** origami
200	12.3±6.7	72.1±6.8	14.3±11.6
300	13.8±3.8	61.2±2.0	25.0±1.9
350	9.9±2.8	73.4±2.1	17.7±4.5
400	7.9±1.5	61.0±2.5	31.0±3.9
500	17.9±6.1	31.4±13.7	50.7±16.4
700	7.2±1.5	17.0±8.6	75.8±9.6
1000	3.5±1.8	9.5±4.8	87.1±6.5

Table S4. Origami binding statistics (mean±SD %) for nanosphere diameters of 200–1000 nm in **Fig. 3O**.

S10. Supplementary Movie

Movie S1. Raw DNA–PAINT data at 100 fps showing transient, stochastic binding of 5 nM P1 imager strands with DNA origami patterned at a 350-nm pitch (300 ms exposure, 13,000 frames).
Refer to zip archive: `Origami designs+staples+movie.zip` for an `.avi` file.